Display Copy

CLM-P220

United Kingdom Atomic Energy Authority

RESEARCH GROUP

Preprint

REVIEW OF EXPERIMENTAL STUDIES OF COLLISIONLESS SHOCKS PROPAGATING PERPENDICULAR TO A MAGNETIC FIELD

J. W. M. PAUL

Culham Laboratory
Abingdon Berkshire

1969

UNCLASSIFIED CLM - P 220

REVIEW OF EXPERIMENTAL STUDIES OF COLLISIONLESS SHOCKS PROPAGATING PERPENDICULAR TO A MAGNETIC FIELD

J.W.M. PAUL

(To be published in the proceedings of the ESRIN Study Group on Collision-free Shocks in the Laboratory and Space. Frascati, June, 1969)

A B S T R A C T

After an introductory discussion of the nature of collisionless shocks, this paper provides an informal review of the current state of experimental studies and their relation to theoretical predictions.

U.K.A.E.A. Research Group,
Culham Laboratory,
Abingdon,
Berks.

September, 1969

CONTENTS

1. INTRODUCTION

Plasma shock waves occur in various astrophysical and space phenomena. Satellite observations have revealed both the earth's bow shock[1,2], resulting from the interaction of the solar wind with the magnetosphere, and also the presence of interplanetary shocks within the solar wind[3]. Optical[4] and radio[5,6] observations of the solar atmosphere have shown that shock waves originate from the flash phase of large flares and can trigger subsequent flares. In addition, shocks are involved in some theoretical speculations about flares[7], pulsars[8,9], quasars[10] and radio-sources[11].

These plasma shock waves are different from those of gas dynamics in that the shock width is much less than the classical mean free path for inter-particle collisions[12]. Hence the name "collisionless" and the search for an explanation of the collisionless increase in entropy[13]. This problem has stimulated much theoretical and experimental interest.

This collisionless heating is thought to result from the following sequence of processes. The plasma in the shock front develops a micro-instability (i.e. growing plasma waves). The non-linear phase of this instability leads to plasma turbulence (i.e. a supra-thermal level of partially random fluctuations). The fluctuating electric field in the turbulent plasma can produce stochastic heating of the particles.

The most difficult theoretical problem is the development of quasi-linear and non-linear theories of plasma micro-instabilities[14–22]. The difficulty of this problem makes guidance from experiment essential.

Experiments have been constructed specifically to study the physics of collisionless shock waves. These have yielded measurements of the variation of density, electric and magnetic fields through the shock and the resulting plasma heating. For one particular type of collisionless shock, recent measurements have demonstrated the presence of plasma micro-instability, with a supra-thermal level of fluctuation, within the shock front. The level of fluctuation appears to be sufficient to explain the observed collisionless heating.

This paper provides an informal review of the current state of experimental studies and their relation to theoretical predictions.

2. PLASMA SHOCK WAVES

Rapid compression of a plasma results in the formation of a steepening wave. This steepening can be limited either by the dispersive nature of the waves (i.e. ω not proportional to k) or by dissipation (irreversible heating) in the large gradients which develop.

Dispersion results in either (a) increasing or (b) decreasing phase velocity as ω increases. For (a) large amplitude rarefraction waves appear in front of the main compression, while for (b) compression waves appear behind the main compression. Such oscillatory waves involve no irreversible heating and are strictly not shocks. However, the addition of some dissipation can damp the waves to give an oscillatory shock transition dominated by dispersive effects.

Dissipation can limit the steepening when the irreversible heating satisfies the appropriate Rankine-Hugoniot conversation conditions (23). In a strong shock the only two such dissipative processes are viscosity and resistivity. Viscosity involves the longitudinal velocity gradient, i.e. the attempt to interstream in the flow direction.

Resistivity involves the magnetic field gradient, i.e. the interstreaming of electrons through ions in a transverse direction. The dissipation results from the randomizing effects of particle deflections during these interstreaming processes.

These particle deflections are caused by fluctuating electric fields in the plasma. When the deflections sum to a 90^{o} deflection they are called a collision. These collisions are classified, depending on the nature of the fluctuating electric field, as follows.

Classical binary collisions: For a plasma in thermodynamic equilibrium the dominant field fluctuations result from the incoherent motion of single particles. As the motions are incoherent the effect is a sum of binary interactions. If Fourier analysed, such fluctuations would have wavelength $\lambda \leqslant \lambda_D$, the Debye length. The classical transport coefficients are derived from this model[12].

Collective collisions: The plasma flowing through the shock front is far from thermodynamic equilibrium and the classical treatment may not be valid. The free energy, which is present in the various gradients, can frequently couple into the collective degrees of freedom of the plasma. These corresponding to plasma waves with $\lambda \geqslant \lambda_D$. The coupling mechanism, which is a plasma instability, is usually complex. However, if such a mechanism exists, the level of wave fluctuations will rise until limited by non-linear effects. These tend to produce turbulence with random phases. The level of these collective fluctuations $(\lambda \geqslant \lambda_D)$ can exceed the level of the incoherent thermal fluctuation $(\lambda \leqslant \lambda_D)$. The supra-thermal fluctuating electric field can produce a 90^{o} deflection of a test particle (i.e. collective collision) in a time much shorter than the classical binary collision

time. Unfortunately these processes have been given the name "collisionless" and this misnomer has lead to some confusion.

Such collective effects are usually treated microscopically by the Vlasov equation and will consequently be reversible, as are all microscopic processes, including binary collisions. However, the process of averaging to produce macroscopic quantities can produce irreversibility[13]. Alternatively, the collective collisions can be put in the collision term of the Boltzmann equation and fluid-like transport coefficients derived in the usual way. Such coefficients are variously called collective, turbulent, effective or anomalous. In using this fluid approach it is important to remember that there is additional energy in the collective degrees of freedom (i.e. wave energy).

3. PERPENDICULAR SHOCK WAVES

3.1 Nature

There are in general three sound speeds (fast, intermediate, and slow) in a magnetized plasma, and consequently there are three types of shock wave[24,25]. These correspond, to a change of fluid velocity across the shock (shock frame of reference) from super- to subsonic for each sound speed.

For propagation, through a highly conducting plasma, in a direction perpendicular to a magnetic field, only fast shocks can exist. These perpendicular shocks are the simplest type of plasma shock in which the magnetic field is important. The Rankine-Hugoniot[23] conservation relation yield a simple compression of plasma and magnetic field, with B and v (fluid velocity) changing magnitude but not direction. The dispersion properties[26] are dominated by electron inertia

at low β (ratio of particle to magnetic pressure) and ion gyration at high β as shown in Fig.1[27].

The formation of a slow sub-shock within the fast shock structure will be discussed in section 6.3. This possibility arises because resistivity allows the plasma within the fast shock to decouple from the magnetic field.

The relative simplicity of the perpendicular shock and the relative ease of experimental study has led to a greater number of publications and a greater understanding than for other types of shock.

3.2 Production

Perpendicular shocks are usually produced in a z or θ-pinch by the cylindrical compression of an initial plasma immersed in an axial magnetic field (B_z). The parameters of the main experimental devices are given in Table I. The main problems, which have to be noted for each experiment are;

(i) Uniformity of initial condition

(ii) Formation of quasi-steady shock (i.e. shock velocity and profile constant for an appreciable time)

(iii) Clear separation of piston (driving magnetic field) from the shock

(iv) Effects of cylindrical convergence

3.3 Measurements

In most experiments the initial conditions (e.g., electron and neutral densities $n_e(R, z)$, $n_n(R, z)$; electron and ion temperatures $T_e(R, z)$, $T_i(R, z)$; $B_z(R, z)$) are resonable well known. Fewer experiments give details of the dynamics (e.g. piston velocity and position $V_p(R)$, $R_p(t)$, shock velocity and position $V_s(R)$, $R_s(t)$).

The shock jumps, ΔB_z, Δn_e, and ΔV_R (radial potential), have been measured in most experiments. However reliable measurements of ΔT_e are available in only a few cases and ΔT_i has not been measured directly[1].

These measurements of the initial conditions, the dynamics and the shock jump provide the starting point for a study of the macrostructure of the shock front. In all experiments one or more of the parameters, $B(t)$, $V_R(t)$, $n_e(T)$, have been measured. These measurements reveal either oscillatory, monotonic or double structures with characteristic rise time τ_s and width L_s. Not all of the structures are even quasi-steady. The variation of L_s with parameters such as n_e, B_z, V_s, $M_A = V_s/V_A$, where V_A is the Alfven velocity, has not been studied systematically. The spatial variations of the temperatures $T_e(t)$ and $T_i(t)$, within the shock, have not been measured.

The collective fluctuations, which constitute the microstructure of the shock, have been studied in a few experiments. These measurements have been made by using either small electric probes or by the scattering of laser light from the collective density fluctuations.

3.4 Parameters

After fixing the angle between the shock normal and B $\left(\text{i.e. } \theta = \frac{\pi}{2}\right)$, the following important parameters remain.

(a) Initial Conditions

(i) m/M (ii) $\beta_1 = \dfrac{n_e \kappa (T_e + T_i)}{(B^2/2\mu_o)} = \dfrac{1}{\gamma}\left(\dfrac{c_s}{V_A}\right)^2$

---

[1] Preliminary measurements of T_i at Novosibirsk were presented during the conference.

(iii) $\alpha = \dfrac{B}{\sqrt{\mu_o n_e m c^2}} = \dfrac{\omega_{ce}}{\omega_{pe}} = \dfrac{\lambda_D}{r_{ce}} = \sqrt{\dfrac{M}{m}}\dfrac{\omega_{ci}}{\omega_{pi}} = \sqrt{\dfrac{m}{M}}\dfrac{\omega_{ce}}{\omega_{pi}} = \sqrt{\dfrac{M}{m}}\dfrac{V_A}{c}$

where Υ is ratio of specific heats, $c_s = \sqrt{\dfrac{\Upsilon k(T_e + T_i)}{M_i}}$ is the ion sound speed, r_{ce} is electron gyro-radius for the electron thermal velocity, and subscripts c and p refer to cyclotron and plasma frequencies respectively.

(b) Dynamics: Mach numbers, Alfven (M_A), Sonic (M_S), magnetosonic (M)

(i) $M_A = \dfrac{V_s}{V_A}$ (ii) $M_S = \dfrac{V_s}{c_s} = \dfrac{1}{\sqrt{\Upsilon\beta/2}} M_A$;

(iii) $M = \dfrac{V_s}{\sqrt{u_A^2 + c_s^2}} = \dfrac{1}{\sqrt{1 + (\Upsilon\beta/2)^2}} M_A$

(c) Collisionless Criteria

(i) $\dfrac{\tau_{coll}(1)}{\tau_s} > 1$ (ii) $\dfrac{\tau_{coll}(2)}{\tau_s} > 1$

where τ_{coll} is the classical collision time and 1,2 refer to pre- and post-shock.

(iii) $R = \dfrac{\text{observed heating}}{\text{classical heating}}$

(d) Microstructure

(i) $\varepsilon = \dfrac{\text{observed fluctuation level}}{\text{classical fluctuation level}}$

(ii) ω/ω_{pi} and $k\lambda_D$ of fluctuation

4. DISPERSIVE EFFECTS FOR LOW β_1

If, on the time scale of the shock, both classical and collective fluctuation are negligible, then the dispersive effect of electron inertia limits the shock steepening for $\omega \sim \sqrt{\omega_{ci}\,\omega_{ce}}$[28]. This produces oscillations at the rear with[29]

$$\lambda = \frac{2\pi}{\sqrt{M_A - 1}} \left(\frac{c}{\omega_{pe}}\right) \sim \left(\frac{c}{\omega_{pe}}\right)$$

Such oscillatory structures have been observed for low $M_A (\sim 1{\cdot}5)$ at both Novosibirsk[30], in Argon with $n_e \sim 10^{12}$ cm^{-3} (Fig.2), and at Julich[29], in hydrogen with $n_e = 5 \times 10^{13}$ cm^{-3} (Fig.3). In both cases there is appreciable damping and the structures are not steady.

The electron drift velocity (V_d) in such non-linear oscillations is given by

$$V_d \sim \frac{1}{\mu_o n_e e} \frac{B}{L_s} = \sqrt{\frac{M}{m}} V_A = \alpha c$$

Thus, if α approaches unity, relativistic effects provide a limit with $V_d = c$. The above relation specifies

$$L_s \sim \frac{B}{\mu_o n_e e V_d} = \frac{V_A}{V_d} \left(\frac{c}{\omega_{pi}}\right)$$

which for $V_d = c$ becomes

$$L_s = \frac{V_A}{\omega_{pi}} = \alpha \left(\frac{c}{\omega_{pe}}\right)$$

The Novosibirsk group have reported[30] observing a shock in Xe with $V_s \sim 10^3$ km/s at $R = 3$ cm with width $L_s \sim 3$ cm $\sim (V_A/\omega_{pi})$.[/] However, no scaling with ω_{pi} was reported nor was the state of ionization of Xe measured.

In these experiments collective collisions are not important because the instability growth time is comparable with or longer than the transit of the plasma through the shock. If the relevant instability is assumed to have a growth time $\tau_g \sim (1/\omega_{pi})$ and to require N growth times within the shock, then for $V_d < c$ instability will occur

---

[/] During the conference similar results were reported from the Naval Research Laboratory, Washington for an Argon plasma with $n_e \sim 10^{12}$ cm^{-3}

for $\tau_g < L_s/V_A$, that is $\alpha < (1/N)$. This onset of instability has been observed in Argon at Novosibirsk[30] in the form of the change from oscillatory to monotonic structure as shown in Fig.4. The transition occurs experimentally for $\alpha \sim 0{\cdot}1$ (i.e. $N \sim 10$). Effectively these dispersive structures can only be seen at low densities and high magnetic fields.

In conclusion, more information is required about dispersive waves under the following headings:

(i) Steady, well separated structures;

(ii) Scaling of parameters, particularly for the relativistic case;

(iii) A general theory of the relativistic case with $V_d \sim c$ and $r_{ce} < \lambda_D$ for which quasi-neutrality is violated,

(iv) High β dispersive effects.

5. SHOCKS WITH LOW β_1 and $M_A < 3$

5.1 Nature

The damping of the electron inertia oscillations is generally believed to result from the transfer of free energy from the electron current into collective fluctuations. This transfer can occur through the mechanism of a resonance coupling (instability) between the electron drift and either ion or electron plasma waves[31]. The resulting enhanced level of plasma fluctuations scatter electrons and limit the electron drift velocity. This process provides an effective resistivity.

5.2 Experiments

Shocks of this type, $2 < M_A < 3$ and $\beta_1 \lesssim 10^{-1}$, have been studied in many laboratories[29,30,32-53]. The most extensive studies

have been performed at Novosibirsk[30,36,37,48] and the most detailed at Culham[32-34,40-42,45-47,53].

In most experiments the initial conditions are well documented and reasonably uniform. The distribution of neutral atom density, particularly near the walls is not known directly and could influence piston formation and dynamics in some experiments.

The dynamics of the shock generation in the Culham experiment are shown in Fig.5. The large tube diameter (50 cm) gives the advantage that there is time to form a steady shock (Fig.6) separated from the piston by 7 cm and from the reflected shock by 0·7 μs, while still 9 cm from the axis. The formation and convergence stages are clearly seen in Fig.6. The magnetic field profiles agree well with the predictions of the Hain-Roberts 2-fluid, 1-D, M.H.D. code[54]. The measured circuit and plasma parameters are used in the computation but rapid ionization of the neutrals near the wall has to be assumed. This agreement allows the use of the computed T_{cons} (i.e. $T_{e2}+T_{i2}$) behind the shock. Other experiments have used the local V_S and ΔB to obtain T_{cons}.

The jump of electron temperature across the shock has been measured reliably by Thomson scattering of laser light at Culham[41-42], Maryland[44] and for high β_1 at Garching[49,52]/. The Garching measurements, which will be discussed in section 7 are very similar to those from Culham. The Maryland results appear to be peculiar to the experiment and are not so well understood. The measurements at Culham show, Fig.7(a), that for $M_A = 2{\cdot}5$ the shock heats the

/ Similar measurements were reported from Julich and Frascati (CNEN) during the conference.

electrons to T_{cons}, while by inference the ions are not appreciable heated. There are no direct measurements of T_i[/]. Attempts to measure T_i in small tubes are easily confused by the rapid rise of T_i when the shock wave converges on the axis.

5.3 Macro-structure

(a) Shock width

Measurements of the profiles of B_z and V_R through the shock have been obtained in many laboratories. The earliest measurements at Culham[34] are shown in Fig.8(a). Also from Culham[40], Fig.9 shows simultaneous oscillograms of B and V_R with a 1 mm B probe situated 1 cm radially in front of a V_R probe. A similar simultaneous measurement, from Novosibirsk[30] is shown in Fig.10. The lag of V_R behind B (i.e., diffusion of B in front of n_e) in this latter experiment, is evidence for the resistive nature of the shock. Measurements from Garching[49], Fig.11, illustrate the problem of obtaining good separation of shock and piston.

The universal result of all these measurements is a montonic profile with

$$L_s \sim 10(c/\omega_{pe})$$

over a wide range of ω_{pe} for hydrogen and deuterium. The shock rise time is shorter than the final collision time and the electron drift velocity exceeds the ion sound speed. The electron inertia oscillation which should be present according to classical theory are not observed. The non-classical damping corresponds to a resistive

---

[/] Preliminary measurements of T_i at Novosibirsk were presented during the conference

shock with an effective resistivity, η^*, given by

$$L_s = \frac{\eta^*}{\mu_o V_s (M_A - 1)}$$

which is about 100 times the classical value. The effective collision frequency $\nu^* = (n_e e^2/m)\eta^*$ is usually quoted in the range $\nu^* \sim 0{\cdot}1$ to $1{\cdot}0\ \omega_{pi}$, although it is not clear that it depende on ω_{pi}.

This scaling of L_s over a wide range of ion mass M_i (Fig.12) has been reported from Novosibirsk[30]. A dependence consistent with $M_i^{1/3}$ was found[✓] but it is not clear which parameters are held constant nor the state of ionization of the ions. At Julich[29] a dependence of ν^*, (obtained from L_s,) on ω_{pi} was found for hydrogen and argon at similar M_A. Again there must be uncertainty about the state of ionization. Changing from hydrogen to deuterium at half the number density leaves all the measured dynamics (e.g. M_A) of the Culham experiment unchanged. The measured temperature and shock width both double[41,42] leaving ν^* constant, although ω_{pi} changes by a factor 0.5. This scaling is consistent with the dependence quoted by Sagdeev[14] and discussed in section 5.5, namely

$$\nu^* \propto \frac{T_e}{T_i}\frac{V_d}{c_s}\omega_{pi} = \frac{T_e}{T_i}\frac{V_d}{V_{eth}}\omega_{pe} \propto \sqrt{\frac{T_e}{n_e}}\frac{1}{L_s}$$

This scaling experiment, with constant $M_A = 2{\cdot}5$ and ν^*, is shown in Fig.13[45] by plotting L_s against $\sqrt{T_{e2}/n_{e1}}$. Three other points have been added which correspond to shocks with ν^* approximately constant ($\pm$ 10%) but have $M_A = 2{\cdot}5$, $2{\cdot}2$ and $2{\cdot}1$ in ascending order of L_s. For these extra points T_{e2} was obtained from the Rankine-Hugoniot relations and ν^* as above from L_s, V_s and M_A.

✓ This dependence was modified to $M_i^{1/4}$ at this conference.

(b) Radial Voltage

The observed radial voltage jump can be explained in terms of the Hall effect and the gradient of electron pressure[33,34]. In a simplified generalized Ohm's law with plane geometry, the radial equation becomes

$$n_e\, e \frac{dV_R}{dX} + J_\theta \times B_z - \frac{dp_e}{dX} = 0 \qquad (X \equiv R)$$

On integration this leads to

$$\bar{n}_e e \Delta V_R = \frac{(B_2^2 - B_1^2)}{2\mu_o} + (p_{e2} - p_{e1})$$

For the Culham experiment this equation is satisfied for $T_{e2} = T_{cons}$. Another way of stating this result is to evaluate

$$Q = \frac{e\Delta V_R}{\frac{1}{2}M(V_1^2 - V_2^2)}$$

For the Culham experiment $Q = 1$[33,34] demonstrating that the ion motion is accounted for by the electric field without any direct viscous drag. For $Q = 1$, $V_R(X)$ yields the ion velocity (i.e. fluid velocity $V(X)$) and by continuity, the electron density $n_e(X)$.

(c) Non Classical Heating

The classical heating within these shock structures has been computed by step-wise integration of the electron energy equation,

$$\frac{3}{2} n_{e1} V_s \kappa \frac{dT_e}{dX} = n_e(X) \kappa T_e(X) \frac{dV}{dX} + \frac{\eta}{\mu_o^2}\left(\frac{dB}{dX}\right)^2$$

using the known profiles of B and n_e (from V_R). The terms due to electron viscosity were shown to be negligible.

In the Culham experiment the ratio of observed to classical heating, $R \sim 6$ and the classical resistivity has to be increased by

100 to explain the observed heating[41,42,45]. A similar result has been obtained for high β shocks at Garching[49,52].

Thus the measured electron temperatures provide direct evidence for the non-classical (e.g. collective) nature of these shocks. These measurements of the electron heating also yield, for the Culham experiment, a mean effective collision frequency within the shock $\overline{\nu^*} \sim 4 \times 10^9$ Hz ($\sim 0{\cdot}1\ \omega_{pi}$).

5.4 Micro-structure

The fluctuating electric fields which constitute the micro-structure and give rise to the collisionless heating are difficult to observe. Measurements have been reported from Novosibirsk[30] which were obtained from double electric probes with separation 0·5 mm. These indicate the presence of fluctuations with $\omega \sim \omega_{pi}$.≠

An estimate of the fluctuating electric field, $E^2(\omega)$, within the shock could be obtained from measurement of the satellites of certain forbidden lines≠ (e.g. He 2P-nF). In experiments at Maryland[55] such satellites have been observed from the piston but not from the shock.

Direct evidence about the nature and magnitude of the collective fluctuations within the shock has been obtained at Culham[45-47,53] by light scattering. The differential scattering cross-section per electron is given by

$$\sigma(\omega, k) = \frac{\langle \delta n_e^2(\omega, k) \rangle}{n_e} \sigma_e = S(\omega, k)\ \sigma_e$$

≠ Measurements with the separation down to $10\ \mu \sim \lambda_D$ and further discussion of the interpretation of these results were presented at this conference.

≠ This subject was discussed by de Silva at the conference.

where $\langle \delta n_e^2(\omega, k) \rangle$ is the Fourier transform of the density fluctuations, σ_e is the appropriate Thomson cross-section for a single electron. The frequency (ω) and wave vector (k) of the wave responsible for the scattering are directly related to the wavelength shift $(\Delta\lambda)$ of the scattered light and angle (θ) of scattering respectively. The experiment was performed with a ruby laser and at a scattering angle, $\theta = 4{\cdot}5^{o}$ for which $k = k_m = 7{\cdot}1 \pm 2{\cdot}5 \times 10^5 m^{-1}$. This corresponds to the important scattering parameter[56] $\alpha = 1/k\lambda_D$ in the range $4{\cdot}4 > \alpha > 1{\cdot}2$ between front and rear of the shock with $\alpha = 1{\cdot}3$ for the mean conditions (i.e. collective fluctuations with $\lambda > \lambda_D$). Details of the experiment and its interpretation are given in a separate lecture but these can be summarized as follows:

(a) Results

(i) The scattered signal and hence the level of fluctuation is enhanced during the transit of the shock through the laser beam as shown in Fig.14.

(ii) With spectral resolution of 0·08 Å, the observed incident and scattered line widths were 0·08 Å and 0·15 Å respectively (Fig.15). As $\omega_{pi} \equiv 0{\cdot}12$ Å the plasma waves responsible for the enhanced scattering have frequencies $\omega < \omega_{pi}$.

(iii) Measurement of $\sigma(k)$, the cross-section integrated over ω, by comparison with the Rayleigh cross sections of N_2 and Ne yielded

$$\langle \delta n_e^2(k_m) \rangle = 4{\cdot}2 \times 10^{23}\ m^{-3}$$

For the mean shock conditions this corresponds to

$$\sigma(k_m) = 3{\cdot}3 \times 10^{-27}\ m^2, \quad S(k_m) = 430$$

(b) Interpretation

The interpretation of these results can be summarized as follows;

(i) Enhanced collective fluctuations ($\lambda > \lambda_D$) exist within the shock front.

(ii) From the frequency spread ($\omega < \omega_{pi}$) and the knowledge that there can be no appreciable Doppler shifts, the fluctuations can be indentified as ion waves and not electron waves for which $\omega \sim \omega_{pe} > \omega_{pi}$.

(iii) The level of fluctuation is more than two orders of magnitude above the stable level for which $S(k) \leqslant 1 \cdot 0$

(iv) By assuming the simple ion wave dispersion relations ($B = 0$) and a power spectrum of isotropic turbulence[/], an estimate of the upper limit of the total turbulence energy can be place at 10% of the mean electron thermal energy.

(v) By using the simple dispersion relations ($B = 0$) the electric field fluctuations $\langle E^2(k_m) \rangle$ can be derived from $\langle \delta n_e^2(k_m) \rangle$. An effective collision frequency (ν^*) can be derived from an isotropic $\langle E^2(k) \rangle$ by using the Fokker-Planck equation. This is described in a separate lecture. The resulting ν^* depends mainly on the fluctuations with $k \sim 1/\lambda_D$. As this is available from the experiment, ν^* can be estimated without a knowledge of the spectrum. The value thus obtained, $\nu^* \sim 5$ GHz, is in good agreement with the value 4 GHz required to explain the

---

[/] Further measurements obtained during the conference and reported separately have shown that the turbulence is not isotropic

observed electron heating (cf. section 5.3(c)).

In conclusion these results appear to provide the foundations of a self-consistent explanation of these low M_A shocks.

5.5 Collisionless Mechanisms

(a) Nature of Instability

The most probable instabilities, which can transfer the free energy of the electron drift into collective fluctuation, are[14,17-22,31,57]

(i) Electron plasma wave instability which occurs for $V_d \geqslant V_{eth}$ (electron thermal velocity) as a result of ion resonance with the electron waves in the moving electron gas[31],

(ii) Ion plasma wave instability which occurs for $T_e > T_i$ and $c_s < V_d < V_{eth}$ as a result of electron resonance[31],

(iii) 'Bump on the tail' instability for non-Maxwellian electrons in which the high velocity component ('tail') drives an electron plasma wave in the rest of the electron gas[57].

Measurements of V_d from the macrostructure eliminate (i) while the measurement of fluctuations with $\omega \sim \omega_{pi}$ eliminates (iii) and verifies (ii).

However in most experiments $T_{e1} = T_{i1}$ and consequently the favoured ion wave instability requires a 'trigger' mechanism to heat the electrons. In fully collisionless conditions, $\tau_{coll}{}^{(1)} \gtrsim \tau_s$, mechanism (i) is thought, without as yet any evidence, to provide an initial small rise in T_e and then to switch off as (ii) takes over. For the Culham experiment with $\tau_{coll}{}^{(1)} < \tau_s$, it has been shown that classical resistive heating can switch on the ion wave instability[45].

(b) Non-linear Theories of the Ion Wave Instability

There are two main theoretical approaches to the ion wave instability problem.

(i) Homogeneous plasma theory of Kadomtsev and Sagdeev

Kadomtsev[18] assumes a constant linear growth rate for ion wave instability in a homogenous steady plasma with $B = 0$. He balances this against non-linear scattering of the waves on ions. This scattering removes energy from the high $k(\sim 1/\lambda_D)$ unstable regions and diffuses it towards an infinite sink at $k = 0$. The balancing process results in a spectrum of turbulence[≠]

$$\langle E^2(k)\rangle = \frac{(2\pi)^3}{7}\left(\frac{V_d}{V_{eth}}\right)\left(\frac{T_e}{T_i}\right)\frac{1}{\psi^2}\frac{(\kappa T_e)^2}{4\pi e^2}\frac{1}{k}\ln\left(\frac{1}{k\lambda_D}\right)$$

spread over a conical region of k (Cerenkov cone for emission of phonons) with axis along $\bar{v}_d$ and half angle $\psi = \cos^{-1}(c_s/V_d)$. This theory has been criticized on the grounds that (i) electron scattering is greater than ion scattering (Drummond[58])[≠] and (ii) magnetic and inhomogeneity effects are important (Krall[59]).

This predicted level of fluctuation, when converted to $\langle \delta n_e^2(k)\rangle$ through the dispersion relations, can be compared with the measurements at Culham. Substitution of experimental values and $T_i = 1{\cdot}7$ eV (adiabatic heating with $\Upsilon = 5/3$) yields

$$\langle \delta n_e^2(k_m)\rangle = 1{\cdot}2 \times 10^{24}\ m^{-3}$$

≠ This formula was taken from ref.18 p.71 by combining $E^2_k = k^2 I_k$ and the formula for I_k. The factor $(2\pi)^3$ appears from converting the Fourier transform to the form used in light scattering theories. A different formula appears in ref 20 p,127.

≠ At this conference Sagdeev stated that Galeev has shown that electron scattering was not greater.

This is about three times the measured value[53].

Sagdeev[19] has used quasi-linear theory to derive an effective collision frequency (ν^*) from the Kadomtsev spectrum and obtained the well known formula[f]

$$\nu^* = 10^{-2} \left(\frac{V_d}{c_s}\right) \cdot \left(\frac{T_e}{T_i}\right) \omega_{pi} = 10^{-2} \left(\frac{V_d}{V_{eth}}\right) \left(\frac{T_e}{T_i}\right) \omega_{pe}$$

Substitution of experimental values for the Culham experiment (mean shock conditions and adiabatic ions with $\Upsilon = 5/3$) yields[47]

$$\nu^* = 1{\cdot}4 \times 10^{10} \text{ Hz}$$

which is about four times that derived from the observed heating (cf. section 5.3)

The step-wise computation of the resistive heating through the shock at Culham (cf. section 5.3) has been extended in include a non-classical resistivity. An effective resistivity, derived from the above ν^*, was added to the classical value for steps in which the linear stability conditions for ion waves[26] were violated. This computation yielded agreement[45] with the measured heating for a collective collision frequency of half that given by the Sagdeev formula. This is roughly consistent with fact that the observed level of fluctuations $\langle \delta n_e^2(k) \rangle$ was a third of that given the Kadomtsev formula.

Although not stated in the paper, the numerical factor 10^{-2}, given by Sagdeev, appears to be a fitting parameter used to bring the

---

[f] This formula appears in reference 20, on p.130 without the factor 10^{-2} and on p.153 without this factor and with c_s replaced by v_{eth}

Kadomtsev spectrum more in line with experiment[≠]. Consequently numerical agreement with this formula, which is frequently noted, may not be of such great significance. However, the scaling, noted in Fig.13, is consistent with the dependencies.

The stochastic method used at Culham[53] to derive ν^* from the experimental $\langle \delta n_e^2(k) \rangle$ has been applied to the Kadomtsev spectrum. This calculation yields a formula for ν^* which is almost the same as that of Sagdeev (with the 10^{-2}).

(b) Inhomogeneous plasma theory of Krall

This theory[21,22] considers the more realistic condition of plasma flow through a shock front. Electron drift motions due to ∇B, ∇n and $E \times B$ are included. The stability of waves propagating in the $X,Y(\equiv R,\theta)$ plane (i.e. perpendicular to B) is considered. The resonance of these waves with the electron drift results in ion wave instability. As a consequency of the plasma flow, the unstable waves have both k_x and k_y components. Linear instability theory yields a maximum growth rate

$$\gamma = \sqrt{\omega_{ce}\ \omega_{ci}}$$

in the region

$$\left(\frac{1}{\sqrt{2}r_{ce}}\right) < |k| < (1/\lambda_d)$$

and with $k_y < k_x$.[≠]

The next step is to assume that within this unstable range there

---

[≠] This was clear from Sagdeev's paper at this conference, in which he also gave an indication of how it might be possible to account for the discrepancy.

[≠] According to discussion during the conference for most experiments $k_\theta \sim 1/r_{ce}$ spread over a range of k_R from $1/r_{ce}$ to $1/\lambda_D$.

is white noise growing at a rate Υ. The effect of this on the electron distribution function is obtained from quasi-linear theory. The effective resistivity ν^*, which is defined[≠] in terms of

$$\int v_y \frac{\partial f_o}{\partial t} d^3v \quad ,$$

can be obtained from this quasi-linear treatment in the form,

$$\nu^* = \sqrt{\omega_{ce}\ \omega_{ci}} \left[\frac{\omega_{pe}^2\ \beta}{\varepsilon^2 c^2}\right] G \ln\left(\frac{1}{a^2}\right)$$

where G is the ratio of the wave to the electron thermal energy, and $\varepsilon = \frac{1}{B}\frac{dB}{dx}$

This collision frequency has been evaluated by assuming,

(i) $v_D \sim v_{eth}$ which reduces the square bracket to unity (N.B. Experimentally $v_D \sim 0{\cdot}1\ v_{eth}$)

(ii) $G \sim 0{\cdot}75$[≠] (N.B. Some experimental indication that for waves in θ direction $G \lesssim 0{\cdot}1$)

These assumptions were made to obtain reasonable agreement with experiment. This comparison with experiment, Table II, was made by substituting ν^* into the usual resistive L_s to obtain

$$L_s = \left(\frac{c}{\omega_{pe}}\right) 0{\cdot}75 \ln\left(\frac{1}{a^2}\right)$$

The agreement on scaling with a is considered significant. However the high level of ion wave fluctuation observed for $k_\theta \sim 1/\lambda_D$ at Culham is contrary to the predictions of this theory.

[≠] On this model quasi-linear limitation leads to $\partial f/\partial t = 0$ and consequently $\nu^* = 0$. This occurs because the electron motion is non-dissipative.

[≠] In the discussion at this conference it appeared that $G \sim 0{\cdot}5$ corresponds roughly with quasi-linear limitation.

5.6 Discussion

There is a clear need for scaling experiments to establish the dependencies of L_s and hence ν^*. In particular the dependence on M_i can be obtained unambiguously by using U.V. preionization which gives only one stage of ionization.

Further measurements of the level and spectrum of turbulence are important for distinguishing between the two existing theories of ion wave turbulence and for developing new theories. A clear and more up-to-date statement of these existing theories with all the assumptions would be most valuable.

6. CRITICAL MACH NUMBER FOR LOW β_1

6.1 Nature of the Effect

Although the change of shock structure at $M_A \sim 3$, was observed as far back as 1965[33,34], there is still no satisfactory explanation. The narrow structure with $L_s \sim 10(c/\omega_{pe})$, which is observed for $M_A < 3$, 'grows' a broad 'foot' with $L_s \sim 2(c/\omega_{pi})$ in front, for $M_A > 3$. This double structure is shown in Figs.8(b) and 16 from Culham[33,34] and Fig.17 from Novosibirsk[30]. There is no direct evidence for dependence of L_s on ω_{pi}. The ratio of the V_R jump across the broad to the narrow features is plotted in Fig.18 from Culham to show $M^* \sim 3$ and that above $M_A \sim 6$ the narrow feature disappears (also shown as Fig.16).

Several different models are used to explain the effect. The relations between them is not clear.

6.2 Limit of Resistive Heating

As M_A increases the amount of plasma heating, required by the Rankine-Hugoniot relations, increases rapidly but the jump of magnetic

field tends to a limiting value. The resistive heating, which is dependent on the magnetic jump, must fail to satisfy the Rankine-Hugoniot relations above some critical M_A. Above this value viscosity, the only other relevant transport coefficient, must also be important.

6.3 Formation of Viscous Sub-Shock

In the reference frame of the resistive shock the plasma flow changes from super to sub-magnetosonic (fast sound speed) on passage through the shock (i.e. fast shock). However on a scale length shorter than the resistive diffusion length in the shock, the plasma is effectively decoupled from the magnetic field. In these circumstances the relevant sound speed is the slow sound speed (c_s). If the plasma enters and leaves the shock supersonically relative to c_s there is no need for a sonic shock. However if the plasma enters supersonically and leaves subsonically relative to c_s then, there must be a sonic, that is slow viscous, sub-shock within the resistive structure. This change occurs at a critical Mach number[60], $M_A = 2{\cdot}76 \sim 3$ for normal experimental conditions ($\beta \ll 1$), and for $M_A > 3$ a sub-shock should occur towards the rear of the resistive shock.[*]

6.4 Critical β

As M_A increases, so does the β within the shock irrespective of β_1. The nature of the dispersion in the plasma (Fig.1) changes for $\beta \sim 1$ in such a way as to produce forward waves with a characteristic length like (c/ω_{pi})[27].

---

[*] At this conference both Drummond and Sagdeev suggested that over a limited range of M_A sub-shock at the rear could be a damped electrostatic wave train resulting from dispersive effects. The electrostatice field if sufficiently large could then reflect the ions.

6.5 Reflection of Ions

The voltage across the resistive shock slows down the incoming ions as described in section 5.3. If the spread of ion velocities (i.e. T_i) and the voltage are sufficiently large, an appreciable number of ions will be reflected forwards. The reflected ion will gyrate in front of the shock gaining energy in the transverse electric field until they passed over the potential barrier into the rear of the shock. This type of process would give a forward characteristic length $L_s \sim r_{ci} \sim (c/\omega_{pi})$. However it is not immediately clear why and how the onset of appreciable reflection should be related to a critical M_A^*. For the observed foot structure at $M_A = 3{\cdot}7$ in Fig.8(b) only a few per cent of the ions should be reflected.

7. SHOCKS WITH LOW β_1 and $M_A > M_A^* \sim 3$

7.1 Experimental Results

The study of high M_A shocks is difficult because L_s increases with M_A as shown in Fig.19 from Culham[45] and because the relative separation of piston and shock decreases. The profile for $M_A = 6.3$ shown in Fig.16 is neither steady nor well separated from the piston.

The double structure obtained for intermediate $M_A = 3{\cdot}7$ at Culham, is reproducible and steady as shown in Fig.20[45]. Unlike most other experiments, this shock can be observed for times $t \sim \tau_{ci} \sim 800$ ns. The 'foot' became steady some 300 ns after its

appearance[4]. The electron heating within the foot, shown in Fig.7(b) is five times the calculated classical heating. Unfortunately there is no direct evidence concerning ion heating. However the difference between the theoretical conservation temperature and the measured electron temperature increases with M_A as shown in Table III. A similar result, for $\beta > 1$, has been obtained at Garching[49,52].

The collective scattering experiment[29] did not detect fluctuations comparable with those at $M_A \sim 2{\cdot}5$. However this may be because a different region of the wave spectrum, in terms of $k\lambda_D$, was observed.

At Novosibirsk[30] electric probe measurements of fluctuations within the foot indicate frequencies $\omega \sim M_A \sqrt{\omega_{ce}\, \omega_{ci}}$. Direct evidence for the reflection of ions into the foot has also been obtained at Novosibirsk. Fast neutrals resulting from charge exchange, have been detected at the wall. The direction and time of arrival of these neutrals show, as in Fig.21 that they originated in the 'foot' when at $R = 2$ cm. The direction and energy (150 eV) of the neutrals indicates that they are moving against the plasma flow as would be expected for a reflected ion gyrating back towards the shock.

7.2 Discussion

There is very little experimental evidence which points to the origin of the broad structure. The measurements at Novosibirsk show that the reflection process is occurring. There is no evidence for a sharp sub-shock at the rear, but it is not clear that such a structure could be resolved anyway. As with low M_A, there are no good

---

[4] Robson suggested that the presence of electric fields reduces the gyration time in the foot to $0{\cdot}25\ \tau_{ci}$ (~ 200 ns here).

scaling experiments and no good measurements of T_i[/].

Theoretical attempts have been made to reconcile the various models mentioned in section 6, but without much success. The current idea appears to be that the viscous sub-shock at the rear of the resistive shock produces increased ion reflections by reason of increased ion heating. The reflection of ions must drag electrons and B-field forward to form the observed foot. The mechanism of reflection is not clear.

The field is open for both experimenters and theoreticians!

8. SHOCKS IN HIGH β_1 PLASMA

Only two experiments in this range of β_1 have been reported; at Julich[29] for $\beta \leqslant 1$ and $M_A \leqslant 9$ (e.g. Fig.24) and at Garching[49,52] $\beta \leqslant 5$ and $M_A \leqslant 8$, $M \leqslant 4$ (e.g. Fig.25).

Theoretically[61] the critical Mach number M_A^* increases and M^* decreases (slightly) with increasing β. However experimentally there does not appear to be any dramatic change at M_A^*, such as occurs for $\beta \ll 1$. For $M_A < M_A^*$ the structure is similar to that at low β with $L_s \sim 10 \left(\frac{c}{\omega_{pe}}\right)$. For $M_A > M_A^*$ there appears to be a gradual increase in L_s toward (c/ω_{pi}) as M_A increases without the appearance of any double structure. In the Julich experiments fluctuations are observed behind the shock front but as can be seen from both Figs.24 and 25 separation of shock and piston is marginal.

The Garching experiment is particularly interesting in that $T_i > T_e$ throughout the experiment. For these conditions ion waves

---

[/] Direct measurement of T_i by charge exchange, at Novosibirsk, was reported at this conference.

should not be unstable,[1] and neither should electron waves ($v_d < v_{eth}$) unless the electrons are non-Maxwellian. The electron temperature has been measured by scattering of laser light (Fig.24) and T_{i1} measured by Doppler broadening of neutral hydrogen lines; $T_{i1} \sim 35$ eV, $T_{e1} \sim 5$ eV, $\beta_1 \sim 3$ and $T_{e2} \sim 45$ eV. Adiabatic heating of the ions, (density profile was measured by 90^o scattering) yields $T_{i2} \sim 85$ eV. The conservation temperature $T_{cons} = T_{e2} + T_{i2} = 185$ eV so that 55 ev of irreversible ion heating is required. These particular measurements were made with $M \sim 2{\cdot}5 > M^*$, and $L_s \sim 0{\cdot}6 \left(\frac{c}{\omega_{pi}}\right)$. The inferred ion heating for $M_A > M_A^*$ increase with M_A.

Again this field is open for both experimenters and theoreticians.

9. SUMMARY

Some of the most significant measurements of shock width (L_s) are plotted against density (n_e) in Fig.25 (modified from a Novosibirsk paper[30]). Although such a plot against a single parameter neglects many important features, it does illustrate the five main classes of perpendicular shocks.

DISPERSIVE NON-LINEAR WAVES AND SHOCKS

A. Non-relativistic, limited by electron inertia: $L_s \sim c/\omega_{pe}$

Theory is well developed and there are a few experimental observations.

B. Relativistic, limited by $V_d = c$: $L_s \sim V_A/\omega_{pi}$

Theory is not well developed and observations are very preliminary.

[1] Sagdeev suggested during the conference that there was an ion wave branch which was unstable under these conditions.

SHOCK WAVES WITH $\beta_1 \ll 1$

C. $M_A < M_A^* \sim 3 : L_s \sim 10(c/\omega_{pe})$

The macroscopic theory of these resistive shocks is well developed. However the various microscopic theories of the instability and turbulence are not yet established. There is a large amount of experimental data from which a self consistent model based on ion wave turbulence is emerging.

D. $M_A > M_A^* \sim 3 : L_s \sim c/\omega_{pi}$

There has been a recent awakening of theoretical interest in this type of shock. However there is no established theory yet. Experimental data has been accumulated but over a narrow range of parameters.

SHOCK WAVES WITH $\beta_1 \leqslant 1$

E. Both theory and experiment are at an early stage.

TABLE I

PARAMETER OF MAIN DEVICES

Laboratory	Device	R cm	L cm	B_{z1} kg	pre-ionizer	n_{e1} cm^{-3}	T_1 eV	β_1	V_c kv	B_{peak} kG	τ_{rise} μs	Vs cm/μs	M_A	References
Culham	"Tarantula" z pinch	25	100	<2	I_z	10^{14}-10^{15}	1.2	0.04-0.6	30-75		0.5	20-50	2 - 6	32-4, 40-3, 45-7, 53
Novosibirsk	"UN1" θ-pinch	8	30	<2	θ-guns	5×10^{10}-10^{14}	1 - 10	$\ll 1$	-	3	0.2	40-100	1 - 4	30,36,37,48
Garching	θ-pinch	7	60	1	1) U.V. 2) I_θ	10^{12}-$2+10^{13}$ 5×10^{13}-5×10^{14}	2 $T_e \sim 5$ $T_i \sim 40$	10^{-2} $\leqslant 5$	40	12	0.5	20-40	1.6 - 3 < 8	49,52
Julich	θ-pinch	9	45	0.5	I_θ	10^{14}	2	$\leqslant 1$	40	7	0.8		1.3 - 8	29
Maryland	1) θ-pinch (small)	4.5	20	1	I_θ	3×10^{14}	1.4	$\ll 1$	40	5	0.2	15	1.3 - 9	39,43,44,5
	2) θ-pinch (large)	23	100	0.3	I_θ	10^{12} R > 10cm 10^{13} R > 10cm	2	$\ll 1$	500 (?)	3	0.05	50	3	50
Moscow	"UV1" θ-pinch	3	30	<3	I_z	5×10^{11}-6×10^{13}	0.1	$\ll 1$	-	1.5	0.05	50	1.3 - 4.2	35

TABLE II

COMPARISON OF SHOCK WIDTHS FROM KRALL'S THEORY WITH EXPERIMENT[22]

Reference	$\frac{1}{\alpha^2}$	$\frac{C}{\omega_{pe}}$ (mm)	L_s (mm)	$\frac{3}{4}\frac{C}{\omega_{pe}} \ln\left(\frac{1}{\alpha^2}\right)$ (mm)
Paul et el	4×10^3	0·17	1·4	1·1
Kurtmullaev et al	$1{\cdot}5 \times 10^3$	0·8	4	4·5
Alikanov et al	30	0·4	0·8	1·0

TABLE III

COMPARISON OF TEMPERATURES (eV)

M_A	2·5	3·7	6·3
T_e : Measured	44	56	44
T_e : Extrapolated back	46	66	-
$T_e + T_i$: Theoretical	49	84	145

REFERENCES

1. HESS, N.F., SCEARCE, C.S., SEEK, J.B., J. GEOPHYS, Res.69 3531, 1964.

2. FRIEDRICKS, R.W., KENNEL, C.F., SCARF, F.L., CROOK, G.M. and GREEN, I.M., Phys. Rev. Letters 21, 1761, 1968.

3. GOSLING, J.T., ASBRIDGE, J.R., BAME, S.J., HUNDHAUSEN, A.J., STRONG, I.B., J. Geophys. Res., 73, 43, 1968.

4. MORETON,G.E., Astron. J., 69, 145, 1964.

5. WILD, J.P., Conf. on Plasma Instabilities in Astrophysics, Asilomar 1968 (Private communication) and with SHERIDAN, K.V., KAI, K., Nature 218, 536, 1968.

6. LACOMBE,C and MANGENEY, A., Astron. and Astrophys. 1, 325, 1969.

7. STURROCK, P.A., Plasma Astrophysics Summer School at Varenna, 1966, p.168 and Nature 211, 695, 1966.

8. HEWISH, A., BELL, S.J., PILKINGTON, J.D.H., SCOTT, P.F., COLLINS, R.A., Nature, 217, 709, 1968.

9. GINZBERG, V.L., ZHELEZNYAKOV, V.V., ZAITSEV, V.V., Astrophys. and Space Science, 4, 464, 1969.

10. STURROCK, P.A., and FELDMAN, P.A., Astrophys. J. 152, L39, 1968.

11. STURROCK, P.A., Plasma Astrophysics Summer School at Varenna, 1966, p.338 and Nature 211, 697, 1966.

12. CHAPMAN, S., COWLING, T.G., Mathematical Theory of Non-Uniform Gases, Cambridge University, 1953.

13. BUNEMAN, O., Phys. Fluids, Suppl. 1964 p.S3.

14. SAGDEEV, R.Z., Rev. of Plasma Physics 4, 23, 1966.

15. KENNEL, C.P., SAGDEEV, R.Z., J. Geophys. Res., 72, 3303 and 3327, 1967.

16. TIDMAN, D.A., Phys. of Fluids 10, 547, 1967.

17. JUKES, J.D., Rep.on Progress in Physics 31, 305, 1968

18. KADOMTSEV, B., Plasma Turbulence, Academic Press, 1965.

19. SAGDEEV, R.Z., Proc. Symp. in Applied Maths. XVIII, 281, 1967.

20. SAGDEEV, R.Z. and GALEEV, A.A., Lectures on Non-Linear Theory of Plasma, I.A.E.A. Trieste Report IC/66/64, 1966.

21. KRALL, N.A., and BOOK, D.L., Phys. Fluids 12, 347, 1969.

22. KRALL, N. Private communication, Maryland Preprint PP 001.

23. de HOFFMAN, F., and TELLER, E., Phys. Rev. 80, 692, 1950.

24. ANDERSON, J.E. Magnetohydrodynamic Shock Waves M.I.T. Press, 1963.

25. KANTROWITZ, A., PETSCHEK, H.E. M.H.D. Characteristics and Shock Waves in "Plasma Physics in theory and Application", Kunkel W.B., McGraw Hill 1966.

26. STRINGER, T.E. J.N.E. (C) 5, 89, 1963.

27. IIYOSHI, A., Culham Report CLM-R74.

28. ADLAM, J.H., ALLEN, J.E. Phil.Mag. 3, 448, 1958

29. HINTZ, E., I.A.E.A. Conference, Novosibirsk 1968, Paper CN-24/A2.

30. ALIKHANOV, S.G., ALINOVSKI, N.I., DOLGOV-SAVELEV, G.G., ESELEVICH, B.G., KURTMULLAEV, R.Kh., MALINOVSKII, V.K., NESTERIKHIN, Yu., PILSKII, V.I., SAGDEEV, R.Z., SEMENOV, V.N., I.A.E.A. Conference, Novosibirsk 1968, Paper CN-24/A1.

31. STRINGER, T.E. J. Nucl. Energy, C, 6, 267, 1964.

32. PAUL, J.W.M., HOLMES, L.S., PARKINSON, M.J. and SHEFFIELD,J. A.P.S. New York 1964, Culham Laboratory Tarantula Memorandum No.131.

33. PAUL,J.W.M., HOLMES, L.S., PARKINSON, M.J., and SHEFFIELD,J. 7th Int. Confer. Phen. in Ionized Gases, Belgrade, II, 819,1965.

34. PAUL,J.W.M., HOLMES., PARKINSON,M.J. and SHEFFIELD,J. Nature 208 133, 1965.

35. ZOGORODNIKOV, S.P., RUDAKOV, L.I., SMOLKIN,G.E., and SHOLIN,G.V. 7th Int.Conf.on Phen. in Ionized Gases (Belgrade) II 791, 1965 also Kurchatov Reports I.A.E., 645 (1964), 909 (1965), 1263 (1966) corresponding to Culham, translation CTO/155, 355, 356.

36. ISKOL'DSKII, A.M., KURTMULLAEV, R.Kh., NESTERIKHIN, Yu.E. and PONOMARENKO, A.G. J.E.T.P. 20, 517, 1965.

37. KURTMULLAEV, R.Kh., NESTERIKHIN, Yu.E., PILSKI, V.I. and SAGDEEV, R.Z. I.A.E.A. Conference, Culham, 1965, Paper CN-21/218.

38. ASCOLI-BARTOLI, U., MARTELLUCCI, S., and MARTONE,M. I.A.E.A. Conference, Culham, 1965, Paper CN-21/75.

39. GOLDENBAUM, G.C. and HINTZ, E. Phys. Fluids, 8, 2111, 1965.

40. PAUL, J.W.M. First European Conference on Controlled Fusion and Plasma Research, Munich, 10-13 October, 1966.

41. PAUL, J.W.M., GOLDENBAUM, G.C., IIYOSHI, A., HOLMES, L.S., HARDCASTLE, R.A. Novosibirsk Symposium on Collisionless Shock Waves 1967, Culham Preprint CLM P-142.

42. PAUL, J.W.M., GOLDENBAUM, G.E., IIYOSHI, A., HOLMES, L.S., and HARDCASTLE, R.A. Nature 216, 363, 1967.

43. GOLDENBAUM, G.C., Phys.Fluids 10, 1897, 1967.

44. de SILVA, A.W. and STAMPER, J.A. Phys.Rev.Letters 19, 1027, 1967

45. PAUL, J.W.M., Culham Progess Report CLM-PR11 1968.

46. PAUL, J.W.M., DAUGHNEY, C.G., HOLMES, L.S., Inst.Phys. and Phys. Soc. (London) Conference on Plasma Diagnostics, Culham, 1968 (Reviewed Nature 218, 324, 1968).

47. PAUL, J.W.M. Contribution to "Physics of Hot Plasmas", Scottish Universities 9th Summer School, 1968, Oliver and Boyd, Edinburgh.

48. KURTMULLAEV, R.Kh., MASOLOV, V.L., MEKLER, K.I. and PIL'SKII,V.I. J.E.T.P. Letters 7, 49, 1968.

49. CHODURA, R., KEILHACKER, M., KORNER, M. and NIEDERMEYER, H. I.A.E.A. Conference, Novosibirsk, 1968, Paper CN-24/A3.

50 de SILVA, A.W., DUCHS, D.F., GOLDEBAUM, G.C., GRIEM, H.B., HINTZ, E.A., KOLB, A.C., KUNZE, H.J. and VITKOVITSKY, I.M. I.A.E.A. Conference, Novosibirsk 1968, Paper CN-24/A8.

51. YAMANAKA, C., NAKAI, S., YAMANAKA, T., IZAWA, Y., KASUYA, K. I.A.E.A. Conference, Novosibirsk 1968, Paper CN-24/A5.

52. KEILHACKER, M., KORNKERR, M. and STEUER, K.H., Z. Physik 223, 385, 1969.

53. PAUL, J.W.M., DAUGHNEY, C.C., and HOLMES, L.S. Nature 223, 822, 1969 Culham Preprint CLM 201.

54. HAIN, K., ROBERTS, K.V., FISHER, D.L., Private communications, Culham computational notes.

55. KUNZE, H.J., GRIEM, H.R., Phys.Rev.Letters 21, 1048, 1968 and private communication.

56. EVAN, D.E. and KATZENSTEIN, J., Rep. on Prog. in Physics, 32, 207, 1969.

57. JACKSON, J.D., J.N.E.(C) 1, 171, 1960.

58. DRUMMOND, W. Private communication.

59. KRALL, N. Private communication.

60. WOODS, L.C., Plasma Physics 11, 25, 1969.

61. JOURDAN, P. Plasma Physics 11, 57, 1969.

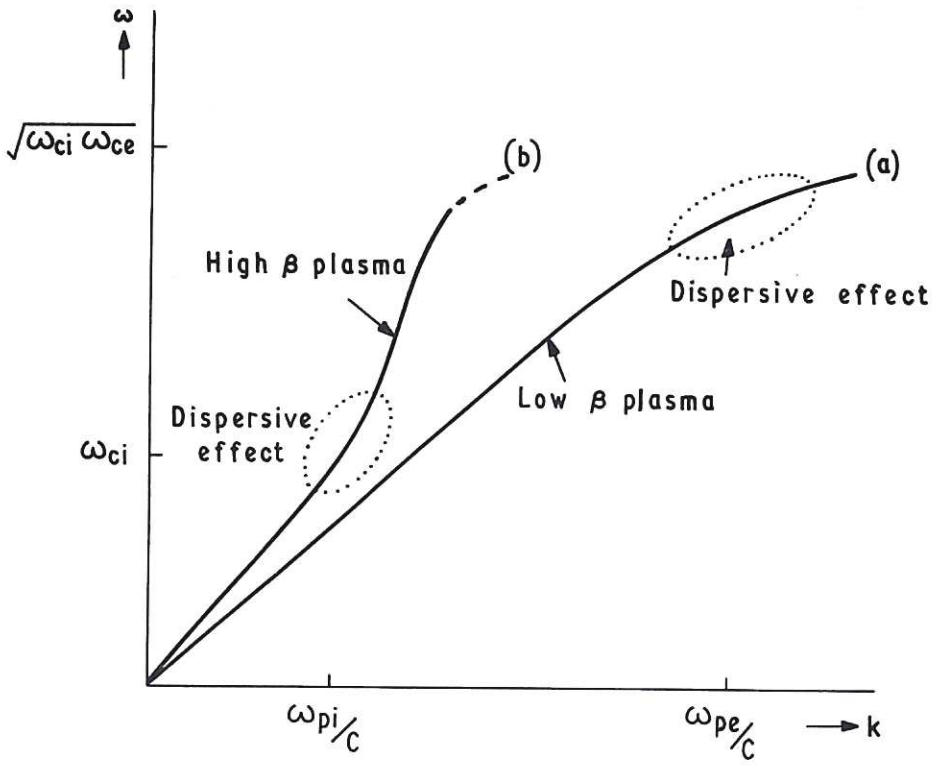

Fig.1 Dispersion for perpendicular propagation[27]
(a) Low β (b) High β

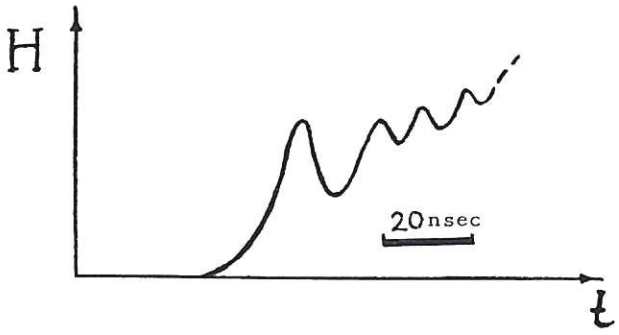

Fig.2 Oscillatory shock front in Argon with $n_e \sim 10^{12}$ cm^{-3} from Novosibirsk[30]

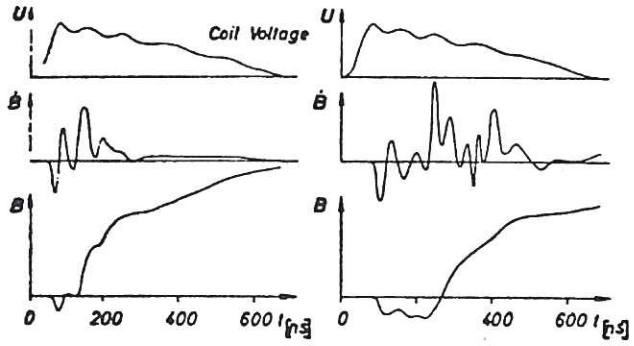

a) Solitary Wave b) Shock Wave

Fig.3 Oscillatory fronts in hydrogen with $B_z = -6$ kG from Julich[29]. (a) Solitary wave for $n_e = 3 \times 10^{13}$ cm^{-3} R = 6 cm (b) Shock wave for $n_e = 5 \times 10^{13}$ cm^{-3}, R = 4 cm, $M_A \sim 1{\cdot}4$

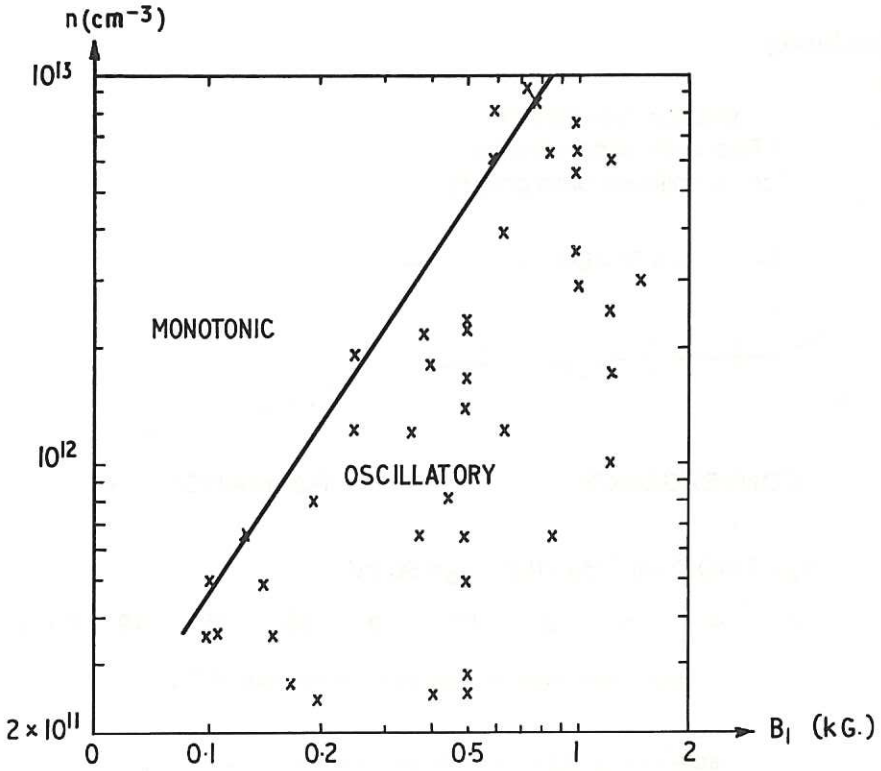

Fig.4 Transition from oscillatory to monotonic shock structure as function of n_{e_1} and B_{z_1} from Novosibirsk[30].

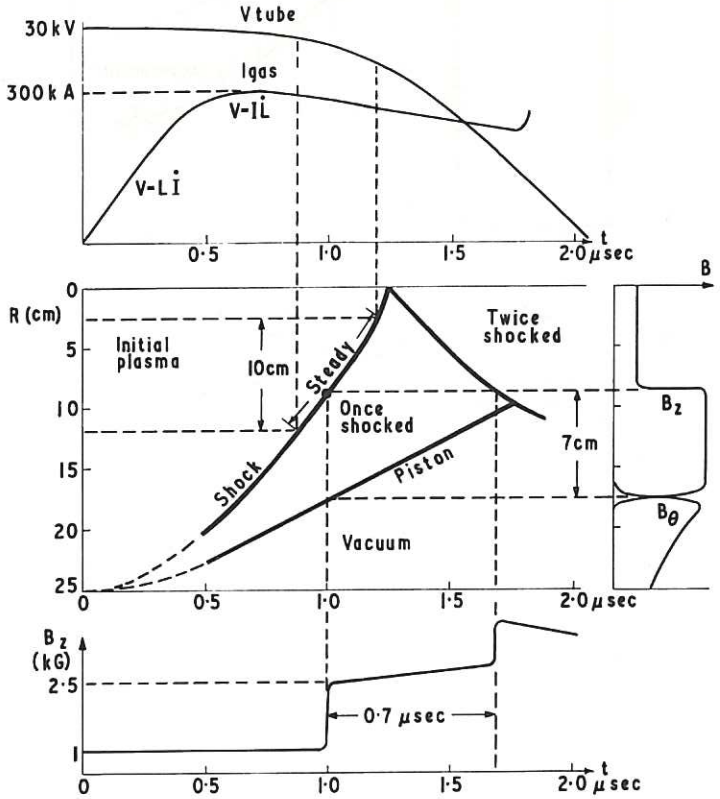

Fig.5 Schematic diagram of dynamics of Tarantula experiment from Culham[47].

CLM-P220

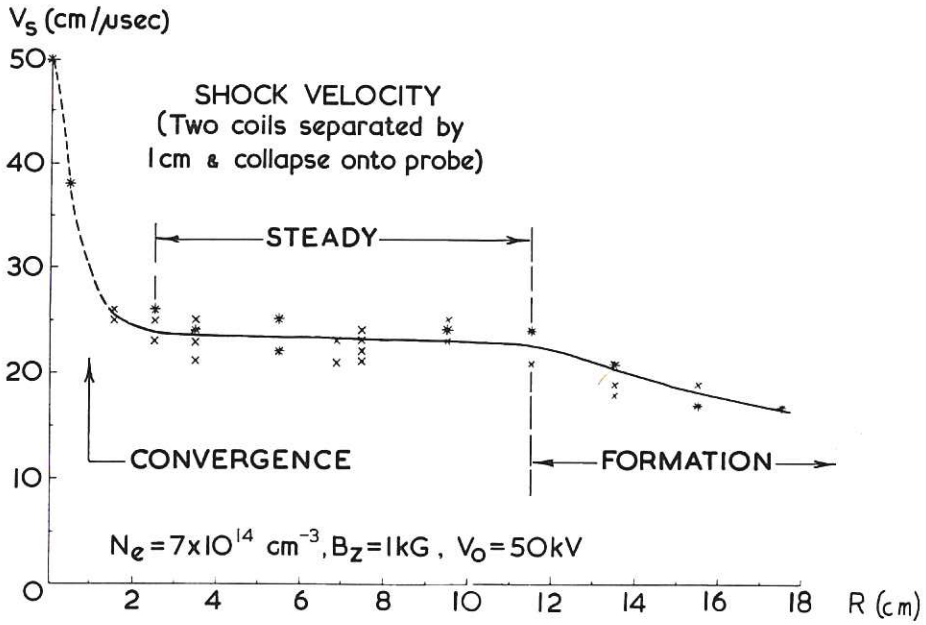

Fig.6 Three stage of shock implosion from Culham[33].

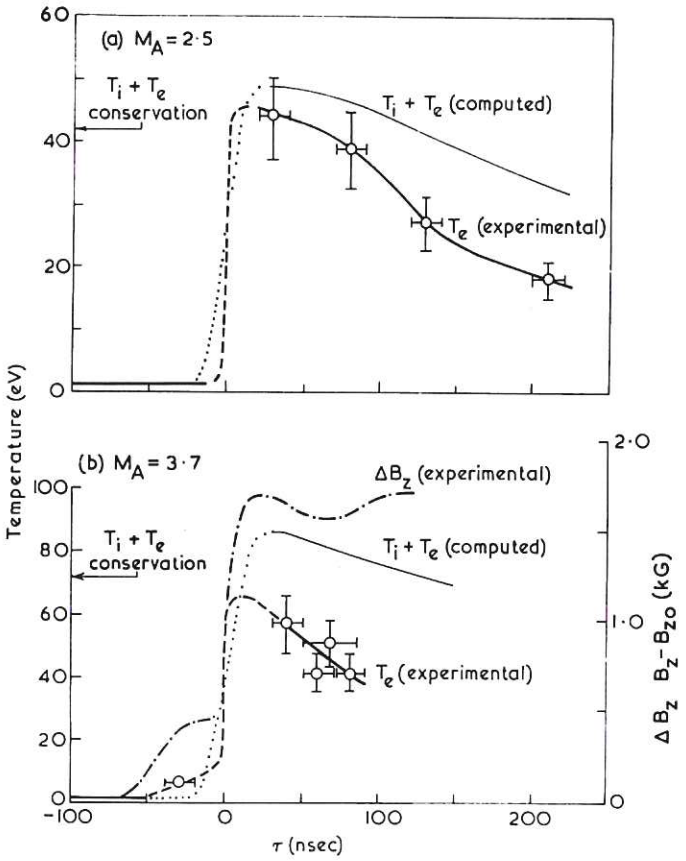

Fig.7 Measured electron temperatures at R = 9 cm in hydrogen with $n_e = 7 \times 10^{14}$ cm^{-3} as a function of time compared with theoretical prediction from Culham[41,42]. (a) $M_A = 2{\cdot}5$, (b) $M_A = 3{\cdot}7$ with $B_z(t)$ plotted to show measurement within "foot".

CLM-P220

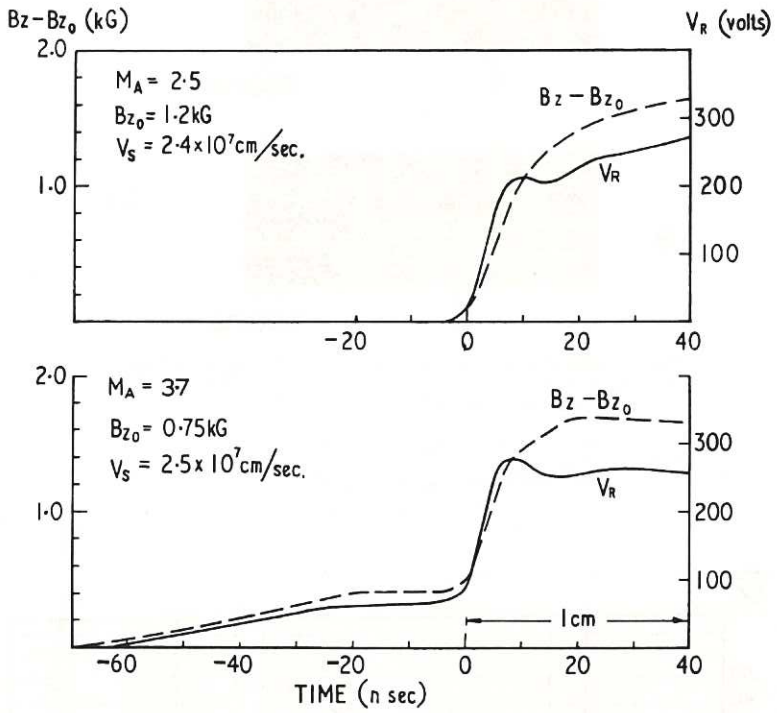

Fig.8 Structure of magnetic field (B_z) and radial potential (V_R) through the shock front for (a) $M_A = 2{\cdot}5$ and (b) $M_A = 3{\cdot}7$. From Culham[33,34].

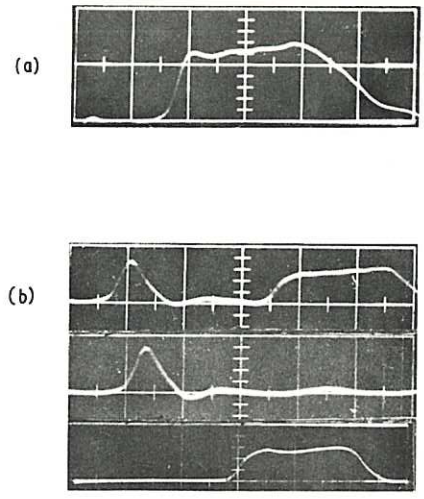

Fig.9
Oscillograph traces of dB_z/dt and V_R from Culham[40].
(a) V_R for $n_e = 1{\cdot}4 \times 10^{14}$ cm^{-3} $M_A = 2{\cdot}1$, $\tau_s \sim 10\ \tau_{ei}$
(b) Simultaneous $\dot{B}$ and V_R from single shot with B probe 1 cm in front of V_R probe for $n_e = 7 \times 10^{14}$ cm^{-3} $M_A = 2{\cdot}5$. On one trace and then on separate traces.

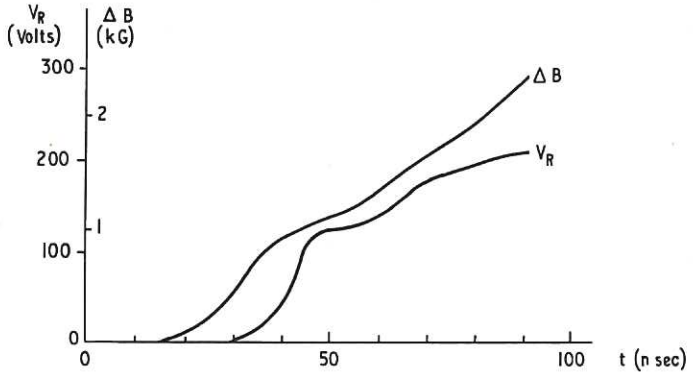

Fig.10
Profile of $\Delta B_z(\Delta H)$ and $V_R(\varphi)$ for hydrogen $n_e = 5 \times 10^{13}$ cm^{-3} from Novosibirsk[30].

CLM-P220

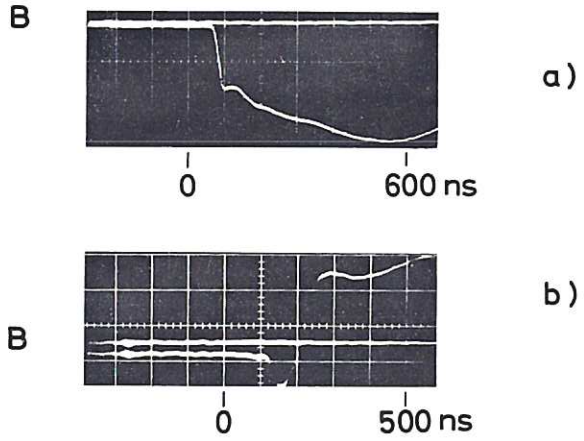

Fig.11 Oscillograms of B_z fro $M_A < M_A^*$, $n_e \sim 10^{13}$ cm^{-3}, R = 2 cm from Garching[49].

(a) Hydrogen $B_{z1} = + 0{\cdot}2$ kG

(b) Deuterium $B_{z1} = - 1{\cdot}0$ kG

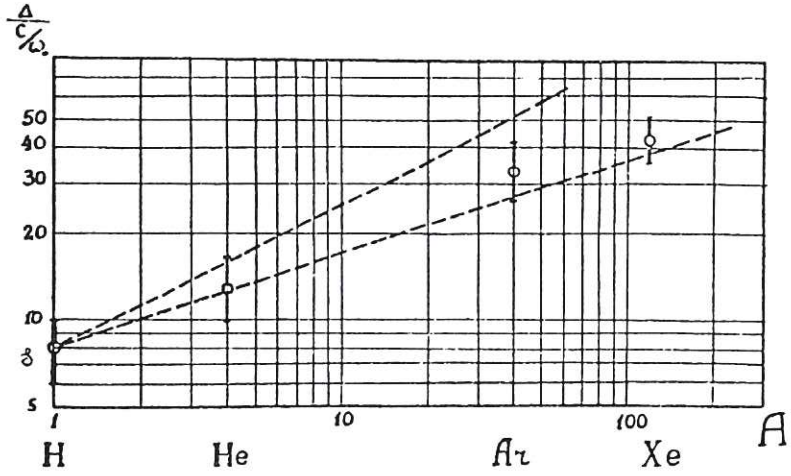

Fig.12 Ratio of shock width Δ to (c/ω_{pe}) for $M_A < M_A^*$ as function of ion mass (A) from Novosibirsk[30].

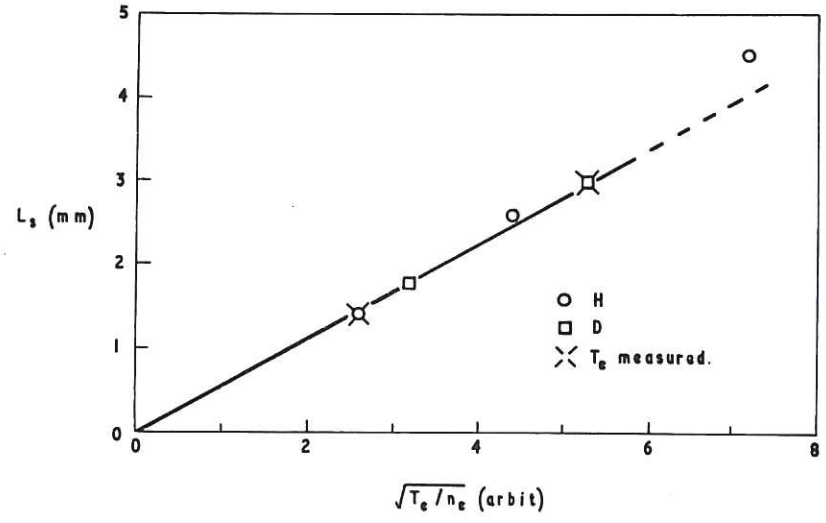

Fig.13 Scaling of shock width L_s for $M_A < M_A^*$ from Culham[45].

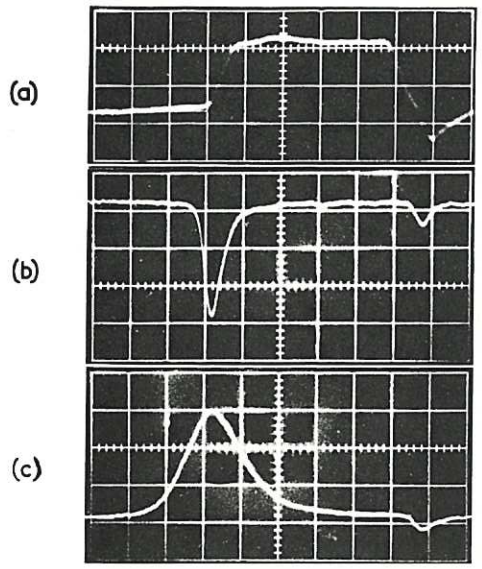

Fig.14
Enhanced forward scattering from shock at R = 9 cm from Culham[53]. Synchronized record of one event with 20 nsec per large division (a) Electric probe monitor of shock, (b) Forward scattered power through 3 Å filter (c) Incident laser power.

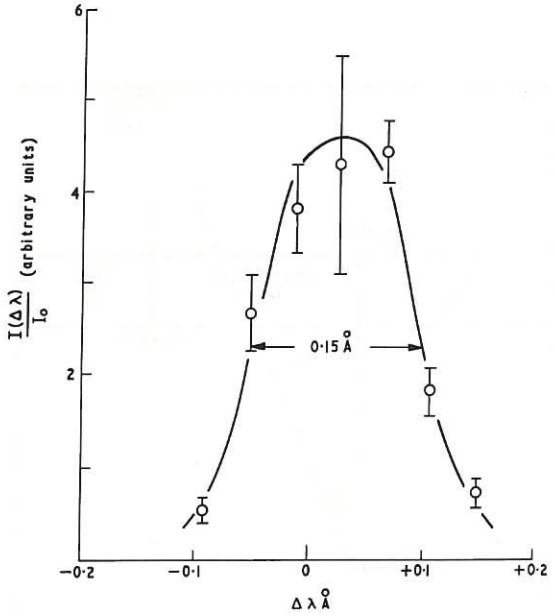

Fig.15
Spectral profile of enhanced scattered light from Culham[53].

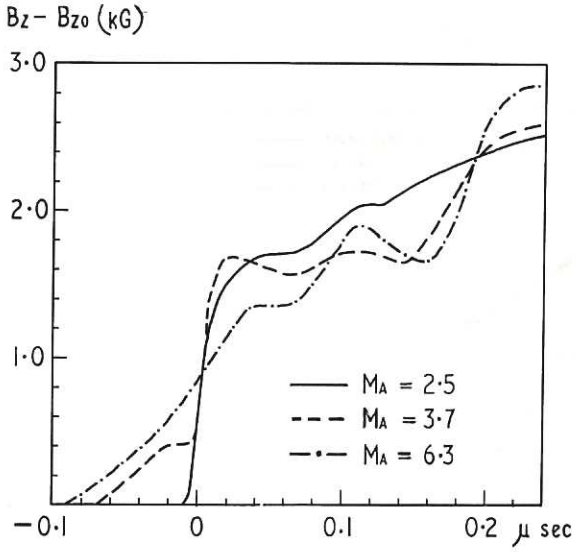

Fig.16
Structure of magnetic field through the shock front from Culham[33,34]
(a) $M_A = 2{\cdot}5$, $n_e = 7 \times 10^{14}$ cm^{-3} $B_{z1} = 1{\cdot}2$ kG
(b) $M_A = 3{\cdot}7$, $n_e = 6 \times 10^{14}$ cm^{-3} $B_{z1} = 0{\cdot}75$ kG
(c) $M_A = 6{\cdot}3$, $n_e = 4 \times 10^{14}$ cm^{-3} $B_{z1} = 0{\cdot}43$ KG

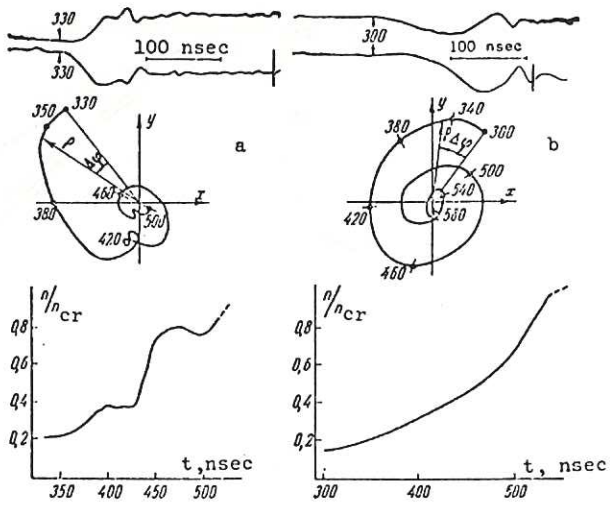

Fig.17
Microwave interferometer signals, hodographs and resulting profiles of n_e for (a) $M_A \sim 3{\cdot}2$, (b) $M_A \sim 4{\cdot}5$ from Novosibirsk[48].

CLM-P220

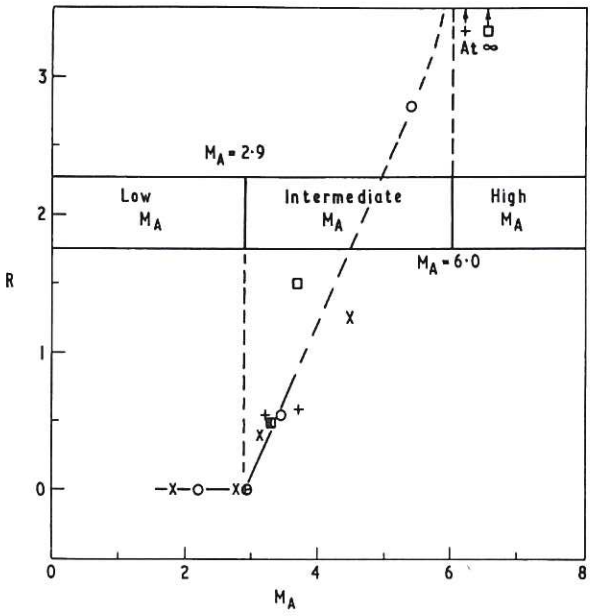

Fig. 18
Variation of ratio (R) of V_R jump across broad to sharp features as function of M_A from Culham[45].

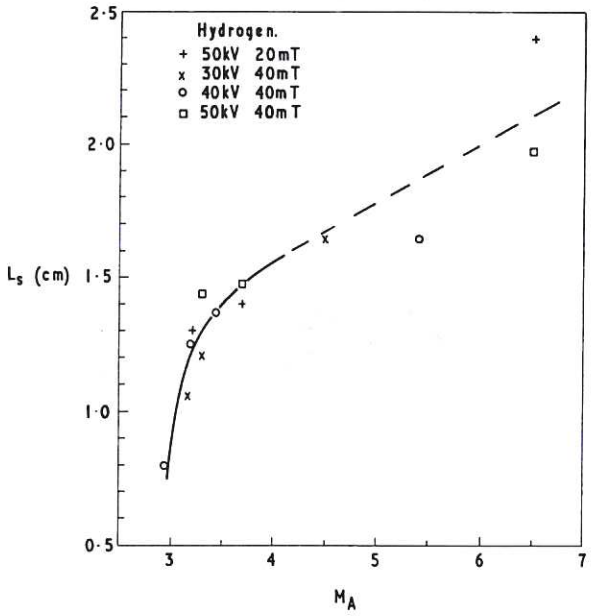

Fig. 19
Scaling of L_s of broad feature with M_A from Culham[45].

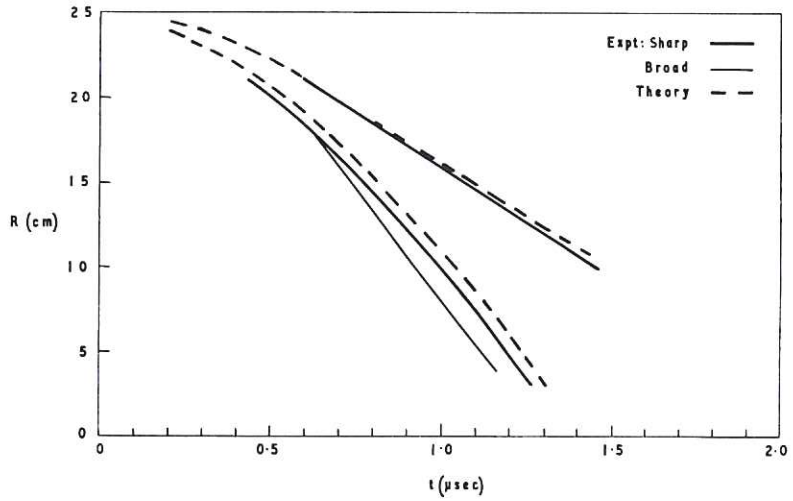

Fig. 20 Magnetic streak diagram of piston and shock for $M_A = 3{\cdot}7$ from Culham[45]. This shows formation of the steady "foot".

CLM-P220

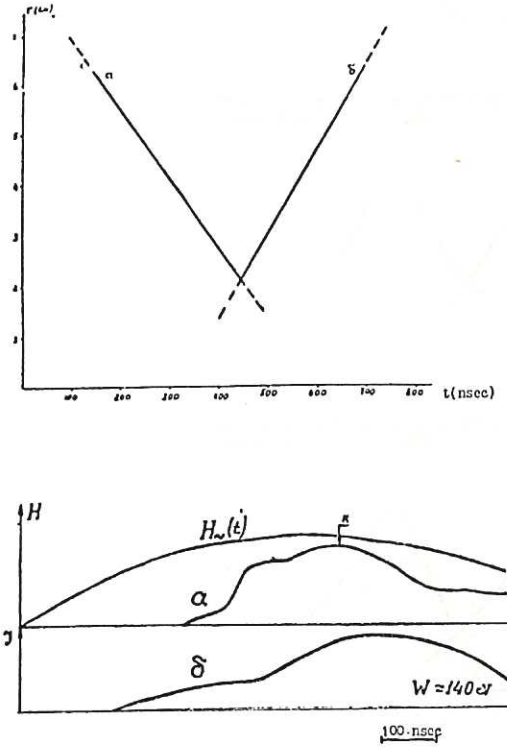

Fig. 21
Measurement of charge exchange neutrals originating in the "foot" from Novosibirsk[30]. Top: Streak diagram of shock (a) and path of neutral (δ) ; Bottom: Trace of applied $B(H_\sim)$, shock B profile (α) and intensity of neutral (δ).

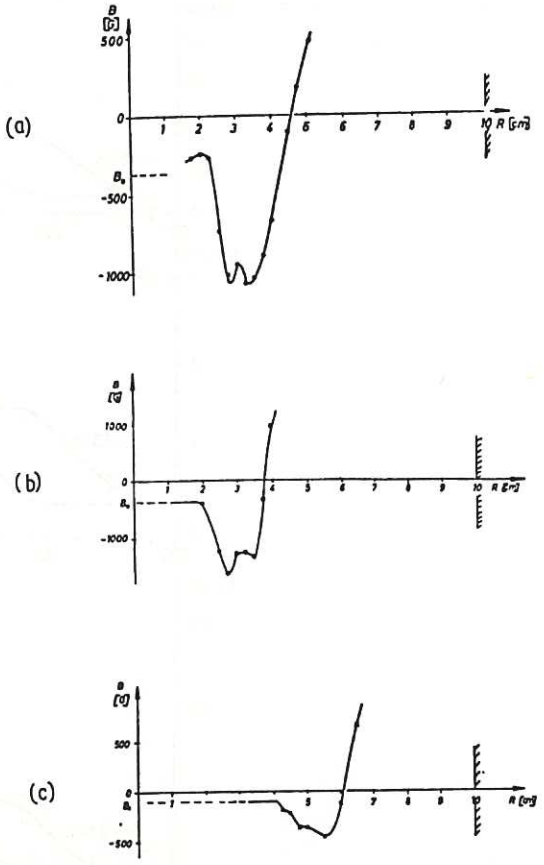

Fig. 22
Shock profiles for high β_i in deuterium from Julich[29]
(a) $\beta_i = 0{\cdot}6$, $M_A = 2{\cdot}7$, $n_e = 1{\cdot}3 \times 10^{14}$ cm^{-3}
(b) $\beta_i = 0{\cdot}6$, $M_A = 4{\cdot}5$, $n_e = 1{\cdot}3 \times 10^{14}$ cm^{-3}
(c) $\beta_i = 1{\cdot}0$, $M_A = 8{\cdot}7$, $n_e = 5 \times 10^{13}$ cm^{-3}

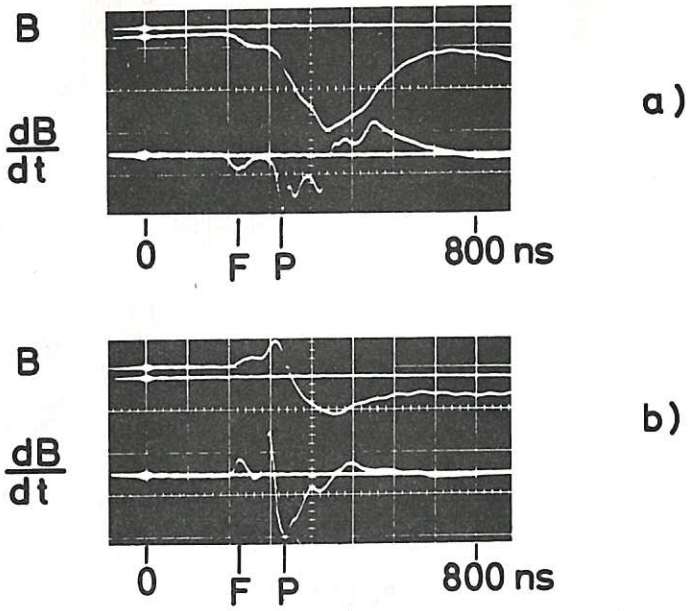

Fig. 23 Oscillograms of B_z and $\dot{B}_z$ at R = 3 cm for high β_i in hydrogen with $n_e \sim 4 \times 10^{14}$ cm^{-3}, $\beta_i \sim 5$, $T_i > T_e$, from Garching[49]
(a) $B_{zi} = +$ 350 G, $M = 2{\cdot}6$, $M_A = 8$
(b) $B_{zi} = -$ 440 G, $M = 3{\cdot}0$

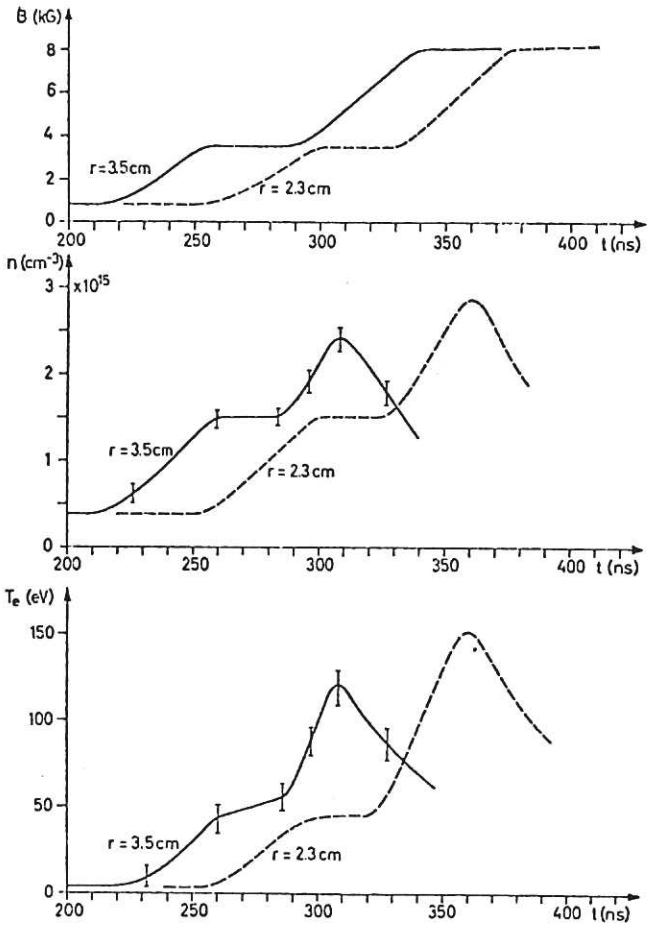

Fig.24 Variation of B, n_e and T_e for $\beta_\perp = 0{\cdot}7$, $M = 2{\cdot}5$, $T_i > T_e$ in deuterium from Garching[47].

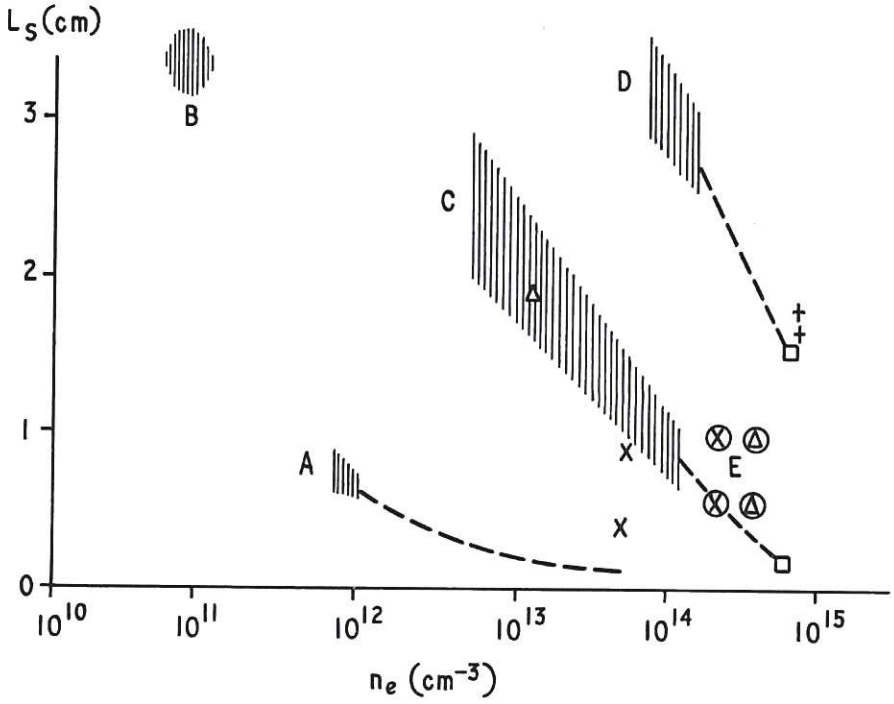

Fig.25 Summary diagram of L_s against n_e based on diagram from Novosibirsk[30].

Novosibirsk	× Julich
□ Culham	+ Maryland
△ Garching	○ High β

CLM-P220

13.11.64